Title (108 characters): Childhood obesity is linked to putative neuroinflammation in brain white matter, hypothalamus, and striatum

Running title (45 characters): Brain microstructure in children with obesity

Authors: Zhaolong Li, BA[1, 2], Amjad Samara, MD[1, 3], Mary Katherine Ray, PhD[1], Jerrel Rutlin, BS[1], Cyrus A. Raji, MD, PhD[3, 4], Joshua S. Shimony, MD, PhD[4], Peng Sun, PhD[4, a], Sheng-Kwei Song, PhD[4], Tamara Hershey, PhD[1, 2, 3, 4, *], Sarah A. Eisenstein, PhD[1, 4]

Affiliations:
[1]Department of Psychiatry, Washington University in St. Louis School of Medicine, St. Louis, MO 63110, USA
[2]Department of Psychological and Brain Sciences, Washington University in St. Louis, St. Louis, MO 63130, USA
[3]Department of Neurology, Washington University in St. Louis School of Medicine, St. Louis, MO 63110, USA
[4]Mallinckrodt Institute of Radiology, Washington University in St. Louis School of Medicine, St. Louis, MO 63110, USA
[a]Present address: Department of Imaging Physics, University of Texas MD Anderson Cancer Center, Houston, TX 77030, USA

***Corresponding author**:
Tamara Hershey, PhD
James S. McDonnell Professor of Cognitive Neuroscience
Department of Psychiatry and Mallinckrodt Institute of Radiology
Washington University in St. Louis School of Medicine
St. Louis, MO 63110
MSC 8134-0070-02
Phone: (314)-362-5593
Email: tammy@wustl.edu

Keywords (5): diffusion MRI; hypothalamus; neuroinflammation; obesity; white matter

Word count in main text: 6080

Abbreviations

ABCD®, Adolescent Brain Cognitive Development℠
ADC, apparent diffusion coefficient
ANOVA, analysis of variance
AUC, area-under-the-curve
BMI, body mass index
CI, confidence interval
DBSI, diffusion basis spectrum imaging
DTI, diffusion tensor imaging
DWI, diffusion-weighted image
FA, fractional anisotropy
FF, fiber fraction
FSL, FMRIB Software Library
FWE, family-wise error
ICV, intracranial volume
MRI, magnetic resonance imaging
NW, children with normal-weight
OB, children with obesity
OW, children with overweight
PDS, pubertal development stage
RF, restricted fraction
RNI, restricted normalized isotropic
RSI, restriction spectrum imaging
SD, standard deviation
SES, socioeconomic status
TBSS, tract-based spatial statistics
TFCE, threshold-free cluster enhancement
WC, waist circumference
WM, white matter

Abstract (200 words)

Neuroinflammation is both a consequence and driver of overfeeding and weight gain in rodent obesity models. Advances in magnetic resonance imaging (MRI) enable investigations of brain microstructure that suggests neuroinflammation in human obesity. To assess the convergent validity across MRI techniques and extend previous findings, we used diffusion basis spectrum imaging (DBSI) to characterize obesity-associated alterations in brain microstructure in 601 children (age 9-11 years) from the Adolescent Brain Cognitive Development^{SM} Study. Compared to children with normal-weight, greater DBSI restricted fraction (RF), reflecting neuroinflammation-related cellularity, was seen in widespread white matter in children with overweight and obesity. Greater DBSI-RF in hypothalamus, caudate nucleus, putamen, and, in particular, nucleus accumbens, correlated with higher baseline body mass index (BMI) and related anthropometrics. Comparable findings were seen in the striatum with a previously reported restriction spectrum imaging (RSI) model. Gain in waist circumference over one and two years related, at nominal significance, to greater baseline RSI-assessed restricted diffusion in nucleus accumbens and caudate nucleus, and DBSI-RF in hypothalamus, respectively. Here we demonstrate that childhood obesity is associated with microstructural alterations in white matter, hypothalamus, and striatum. Our results also support the reproducibility, across MRI methods, of findings of obesity-related putative neuroinflammation in children.

1. Introduction

Childhood obesity is a major growing health issue, affecting over 340 million children worldwide in 2016 (World Health Organization, 2021). It is associated with expensive medical costs (Biener et al., 2020), lower quality of life (Killedar et al., 2020), and elevated risk for health complications including adult obesity, type 2 diabetes, and cardiovascular diseases (Liang et al., 2015; Simmonds et al., 2016). Accumulating evidence also identifies childhood obesity as a risk factor for cognitive dysfunction and Alzheimer's disease in late-life (Tait et al., 2022). Given the brain's prominent role in regulating feeding and metabolism, it is essential to understand the relationship between obesity and brain health. Determining which brain regions and networks might be involved in the development and maintenance of childhood obesity could help identify targets for obesity prevention and intervention, thereby mitigating short and long-term health consequences.

Obesity involves a chronic, low-grade, systemic inflammation affecting multiple organs (Gregor & Hotamisligil, 2011). In rodent models of obesity, high-fat diets induce inflammation in the central nervous system, or "neuroinflammation" (Baufeld et al., 2016; Buckman et al., 2013; De Souza et al., 2005; Décarie-Spain et al., 2018; Valdearcos et al., 2017), which in turn cause memory deficits and anxiodepressive behaviors (Beilharz et al., 2016; Décarie-Spain et al., 2018; Pistell et al., 2010). In humans, post-mortem tissue analyses have revealed associations between obesity and increased gliosis in multiple brain regions, including the hypothalamus, a key regulator of feeding and metabolism (Baufeld et al., 2016; Schur et al., 2015). Aimed at assessing brain health *in vivo*, a number of magnetic resonance imaging (MRI) studies have reported associations between obesity and altered brain structure. In adults, higher body mass index (BMI) and visceral fat are consistently linked to lower cortical thickness and smaller prefrontal and basal ganglia volumes (Fernández-Andújar et al., 2021; Gómez-Apo et al., 2021; Raji et al., 2010; Willette & Kapogiannis, 2015), potentially due to neuronal loss consequent of obesity-related neuroinflammation and/or microangiopathy (Gómez-Apo et al., 2021). These relationships are less clear in children (Willette & Kapogiannis, 2015). Adult obesity has also been associated with compromised white matter integrity, reflected by lower diffusion tensor imaging (DTI)-derived fractional

anisotropy (FA) and greater mean diffusivity of water, primarily in frontolimbic tracts and the corpus callosum (Daoust et al., 2021; Kullmann et al., 2015; Verstynen et al., 2012). However, opposite findings of greater white matter DTI-FA in obesity have also been noted (Birdsill et al., 2017; Carbine et al., 2020; Dekkers et al., 2019), and the relationship between obesity and white matter integrity in children remains unknown. Importantly, the standard single-tensor DTI model could be confounded by neuroinflammatory processes such as cellularity and edema (Kullmann et al., 2016; Wang et al., 2011, 2015; Winklewski et al., 2018), which may partially explain the mixed pattern of results.

In recent years, studies using multi-compartment diffusion MRI-based methods, though limited in number, have yielded consistent observations of putative neuroinflammation in feeding-related brain regions in obesity (Rapuano et al., 2020, 2022; Samara et al., 2020, 2021). The data-driven multi-tensor diffusion basis spectrum imaging (DBSI) technique models diffusion-weighted signals as a linear combination of discrete anisotropic tensors and isotropic diffusion spectra, enabling the *in vivo* assessment of brain microstructure (Cross & Song, 2017; Wang et al., 2011, 2015). DBSI metrics, though indirectly reflecting true anatomy, have been histopathologically validated as neuroinflammation-sensitive using rodent and human neural tissue in multiple sclerosis (Chiang et al., 2014; Wang et al., 2014; Wang et al., 2011, 2015), epilepsy (Zhan et al., 2018), and optic neuritis (Lin et al., 2017; Yang et al., 2021). Notably, applying DBSI to adults with obesity, we previously observed microstructural alterations in striatal and limbic regions that suggest cellularity, vasogenic edema, and lower apparent axonal and dendritic densities (Samara et al., 2020, 2021), in line with the obesity-related neuroinflammatory phenotype seen in animal and post-mortem human brain studies. In white matter tracts, we found evidence of increased and widespread DBSI-assessed putative neuroinflammation in young and middle-aged adults with obesity across two independent samples (Samara et al., 2020). DBSI has not yet been used to characterize brain microstructure in childhood obesity. However, Rapuano et al., (2020) used restriction spectrum imaging (RSI), which in contrast to DBSI, models isotropic water diffusion components based on the ratio of radial and axial diffusivities (Palmer et al., 2022; White et al., 2013), and observed associations between greater purported striatal cellular density and higher baseline

and future waist circumference and BMI in children in the Adolescent Brain Cognitive Development[SM] (ABCD) Study (Rapuano et al., 2020, 2022). Furthermore, using a non-diffusion method, namely quantitative T2-weighted MRI, studies have reported that longer hypothalamic T2 relaxation time and greater T2 signal intensity, both suggestive of reactive microglial and astrocytic gliosis, relate to higher BMI in adults (Schur et al., 2015; Thaler et al., 2012) and children, including a subset from the ABCD Study® (Sewaybricker et al., 2019; Sewaybricker, Kee, et al., 2021; Sewaybricker, Melhorn, et al., 2021). Convergent findings amongst MRI methods in the same group of children would support the feasibility and reliability of these techniques to assess putative neuroinflammation in childhood obesity.

In this study, we used the baseline ABCD Study® data from 601 children aged 9-11 years (see **section 2.1** for details on sample selection) to test the *a priori* hypotheses that 1) obesity-associated microstructural alterations, including greater putative neuroinflammation-related cellularity (reflected by greater DBSI restricted fraction (RF)) and lower axonal and dendritic densities (reflected by lower DBSI fiber fraction (FF)) that we had observed in white matter and striatum in adults, and in one novel region not yet assessed using diffusion MRI, i.e., the hypothalamus, would also be present in children, and that 2) greater hypothalamic and striatal cellularity (DBSI-RF) would relate to greater baseline waist circumference and BMI metrics in children, similar to the RSI cellular density metric, namely restricted normalized isotropic (RSI-RNI). We also explored associations between baseline DBSI and RSI metrics in the hypothalamus and striatum and one and two-year longitudinal changes in anthropometrics. If our results using DBSI are consistent to those in studies that used RSI and quantitative T2-weighted MRI, they will support the use of non-invasive MRI-based methods to characterize obesity-related putative neuroinflammation *in vivo* in humans, in the absence of histopathological validation.

2. Materials and methods

2.1. Participants

Participants were from the ABCD Study®, a ten-year, 21-site study tracking brain development in a diverse cohort of U.S. children and adolescents (Casey et al., 2018; Garavan et al., 2018; Jernigan et al.,

2018). Participants receive annual physical, sociocultural, and behavioral assessments, as well as neuroimaging and bioassays every two years. Institutional review boards at study sites approved study procedures; parents/caregivers provided written consent and children gave verbal assent. The ABCD Study® 2.0.1 release included data from 11,875 participants at baseline and 4,951 participants at one-year follow-up. In addition to the ABCD Study® inclusion/exclusion criteria (Garavan et al., 2018), we excluded participants with 1) missing anthropometric or demographic data at baseline or one-year follow-up; 2) current or past diagnosis of neurological (including cerebral palsy, brain tumor, stroke, aneurysm, brain hemorrhage, intellectual disability, lead poisoning, muscular dystrophy, multiple sclerosis, and others) and psychiatric (including schizophrenia, autism spectrum disorder, attention-deficit hyperactivity disorder, and others) conditions and diabetes, similar to Rapuano et al., (2020); and 3) T1 or diffusion-weighted images (DWIs) that did not pass quality control or had clinically significant incidental findings (Hagler et al., 2019; Li et al., 2021). Also consistent with Rapuano et al., (2020), in order to maximize harmonization of MRI data across sites, only scans performed on Siemens 3T Prisma platforms (Siemens Healthineers AG, Erlangen, Germany) were included. As the ABCD Study® 4.0 release became available during our study, we further included participants with complete data at two-year follow-up to extend exploratory longitudinal analyses. Lastly, because head motion during MRI scans is known to interfere with diffusion tensor model estimation and give spurious correlations (Ling et al., 2012; Yendiki et al., 2014), we excluded participants with excessive head motion (defined as mean DWI framewise displacement ≥ 2.5 mm) and covaried for mean head motion in statistical analyses.

Our inclusion/exclusion criteria selected a total of 1,613 qualifying participants (see **Supplementary Fig. 1** for flowchart). Age and sex-adjusted BMI percentiles at baseline were used to classify participants by weight status (Kuczmarski et al., 2002), including 63 with underweight (BMI < 5th percentile), 1,140 with normal-weight (NW; 5th to < 85th percentiles), 194 with overweight (OW; 85th to < 95th percentiles), and 216 with obesity (OB; ≥ 95th percentile). To achieve balanced group sizes as well as reduce computational cost, we randomly selected 216 NW participants (matched to OB group size) stratified by sex, and included all 194 OW and 216 OB participants. After neuroimaging processing, data

from 25 participants were excluded due to missing/incomplete T1 or DWI acquisition, missing field maps, mismatch between field map and DWI dimensions, or missing/unclear DWI directions. The final analytical sample therefore included 212 NW, 187 OW, and 202 OB participants, for a total $n = 601$. Such sample size is similar to those in recent literature and should afford sufficient power to detect obesity-related microstructural alterations (see **Supplementary Methods** for power analysis) (Jiang et al., 2023; Sewaybricker, Kee, et al., 2021).

2.2. Obesity-related measures

Participant waist circumference (WC), weight, and height were measured at baseline and one and two-year follow-ups (Barch et al., 2018). Raw BMI was calculated ($\text{weight}_{(\text{lbs})}/\text{height}_{(\text{in})}^2 \times 703$). BMI *z*-scores corrected for age and sex were computed using the 2000 CDC growth charts (Kuczmarski et al., 2002). These different measures were used to address the concern that a single index may be less reflective of true adiposity and/or sensitive to fat gain in children (Cole et al., 2005; Taylor et al., 2000).

2.3. Neuroimaging

2.3.1. MRI acquisition

Details on T1 and DWI acquisition and harmonization across sites are published elsewhere (Casey et al., 2018; Hagler et al., 2019). T1-weighted anatomical images were collected as a 3D T1-weighted inversion prepared RF-spoiled gradient echo scan, with voxel resolution = 1 mm^3 isotropic. Spin echo echo-planar imaging was used to acquire multi-shell DWIs with the following parameters: total acquisition time = 7:31, repetition time = 4100 ms, time to echo = 88 ms, matrix size = 140 × 140 × 81, flip angle = 90°, acceleration factor = 3, and voxel resolution = 1.7 mm^3 isotropic. DWIs were imaged with 7 b = 0 frames and 96 gradient directions (b's = 500, 1000, 2000, and 3000 s/mm^2 with 6, 15, 15, and 60 directions, respectively).

2.3.2. DWI and DBSI processing

DWIs were corrected for susceptibility-induced distortion, eddy currents, and head motion using FMRIB Software Library (FSL) *topup* and *eddy* (Smith et al., 2004). Multi-tensor DBSI maps were estimated using an in-house script as previously described (Wang et al., 2011, 2015). Leveraging the

multi-shell DWI data, DBSI characterizes brain tissue microstructure by partitioning the total water diffusion signal within each image voxel into isotropic and anisotropic compartments. DBSI modeling produced maps of anisotropic fiber fraction (DBSI-FF; reflects axonal/dendritic density), isotropic nonrestricted fraction (*f*(D) at apparent diffusion coefficient (ADC) > 0.3 μm^2/ms; reflects vasogenic edema/tissue disintegration/extracellular water), and isotropic restricted fraction (DBSI-RF; *f*(D) at 0 < ADC ≤ 0.3 μm^2/ms; reflects intracellular water/inflammation-related cellularity) (Chiang et al., 2014; Sun et al., 2020; Wang et al., 2015). Details on DBSI model specification are provided in **Supplementary Methods**. Notably, DBSI-FF and RF are consistently lower and greater, respectively, in adult obesity (Samara et al., 2020, 2021) and serve as the neuroinflammation-related microstructural assessment in the current study. DBSI maps were registered to T1 space first using *epi_reg* and a non-diffusion-weighted image, then by applying the transformation matrix to individual maps using *applyxfm*.

2.3.3. Tract-based spatial statistics (TBSS)

Voxel-wise analyses of white matter DBSI-FF and RF were performed using TBSS (Smith et al., 2006). The DTI model was fitted to preprocessed DWIs using FSL *dtifit*, and DTI-FA maps were eroded by one voxel with end slices removed. Cleaned DTI-FA images were nonlinearly registered to the T1-weighted image of a randomly selected NW participant, averaged, and assigned a threshold at FA > 0.2 to create a white matter skeleton, onto which the DBSI-FF and RF maps were projected.

2.3.4. Segmentation of the striatum and hypothalamus

The nucleus accumbens, caudate nucleus, and putamen were segmented from T1-weighted images using FSL *FIRST* (Patenaude et al., 2011). The hypothalamus was segmented using a novel, automated algorithm developed with deep convolutional neural networks trained on adult data (Billot et al., 2020). To assess the algorithm's accuracy in children, we compared automated and manual hypothalamus segmentations in 20 participants (10 NW and 10 OB, randomly selected within each group). Within this group, the automated and manual segmentations had good spatial overlap (mean Dice similarity coefficient = 0.74, *SD* = 0.02, one-tailed $p < 0.001$ against the conventional threshold of 0.7) and yielded highly correlated volumes ($r = 0.74$, $p < 0.001$). Neither spatial overlap nor volumetric

correlation between the automated and manual segmentations was different by weight group (NW vs. OB; p's = 0.58 and 0.97). Although the automated segmentations had smaller volumes than manual segmentations (*means* = 747 and 887 mm^3, $p < 0.001$), such volume reduction primarily excluded voxels near the hypothalamic surface, reducing possible contamination of diffusion signal from neighboring cerebrospinal fluid and vasculature (**Supplementary Fig. 2**). Also, the segmented volumes were consistent with literature values (Neudorfer et al., 2020). Taken together, the automated algorithm reliably produced hypothalamus segmentations comparable to manual segmentation. For each subcortical structure, segmentations were visually inspected for accuracy before statistical analyses, and volume and DBSI-FF and RF metrics were each extracted and combined/averaged between hemispheres.

2.4. Statistical analyses

All analyses, except for TBSS, were performed in R version 4.2.1 (R Core Team, 2013). Differences in participant characteristics across NW, OW, and OB groups were assessed using analysis of variance (ANOVA) or chi-square tests.

2.4.1. White matter

For TBSS, we excluded data from 28 randomly selected siblings, eliminating family dependency confounds. Baseline DBSI-FF and RF in white mater tracts were compared amongst unrelated NW (n = 202), OW (n = 180), and OB (n = 191) participants using voxel-wise TBSS, first by ANOVAs for main effects of group and second by t-tests for between-group comparisons. FSL *Randomize* (null distribution built from 10,000 permutations; with recommended threshold-free cluster enhancement (TFCE)) was used for these comparisons with spatial family-wise error (FWE) rate corrected at two-tailed $p \leq 0.05$) (Winkler et al., 2014). Briefly, the raw statistical image was TFCE-transformed into an output image in which voxel-wise TFCE scores were weighted sums of local clustered signals, such that larger TFCE scores reflected magnitude of cluster-like spatial support greater than a given height (signal intensity) (Li et al., 2017; Smith & Nichols, 2009). We specified the –T2 option in *Randomize* (2D optimization for skeletonized data, cluster height weighted by $H = 2$, cluster extent weighted by $E = 1$, voxel connectivity = 26). Voxel-wise analyses using TBSS and TFCE allowed for sensitive detection of regionally-specific

obesity-related DBSI-FF and RF effects in white matter, while stringently controlling for multiple comparisons across space. Participant age, sex, race/ethnicity, parental education, household income, parental marital status, pubertal development stage (PDS), mean head motion, and intracranial volume (ICV) were covaried in TBSS. Group differences in white matter skeleton-average values of DBSI-FF and RF were assessed with linear mixed-effects models using the *lme4* package (Bates et al., 2015), where the same set of covariates plus weight group were fixed effects and site was the random effect.

2.4.2. Striatum and hypothalamus

DBSI-FF and RF outliers in the nucleus accumbens, caudate nucleus, putamen, and hypothalamus that were ± 3 SD away from the mean were removed (**Supplementary Table 1**). One and two-year changes in obesity-related measures (i.e., WC, BMI, and BMI *z*-scores) were calculated by subtracting baseline from respective follow-up. Extreme BMI values (< 10 kg/m^2 or > 50 kg/m^2) and associated BMI *z*-scores were removed, including 1 NW and 1 OB at one-year and 1 OW at two-year. Distributions for obesity-related measures at and changes between all timepoints are shown in **Supplementary Fig. 3**.

Associations between DBSI metrics and baseline or future change in obesity-related measures were assessed using linear mixed-effects models. Age (at baseline, one, or two-year), sex, race/ethnicity, PDS (at baseline, one, or two-year), parental education, household income, parental marital status, mean head motion, and ICV were covaried due to potential confounding (Lawrence et al., 2022; Li et al., 2023; Palmer et al., 2022; Rapuano et al., 2020), and the random effect was family nested within sites. In longitudinal models, baseline obesity-related measures were also covaried. As we had *a priori* hypotheses, and the goal was to describe regionally-specific relations between tissue microstructure and convergent obesity-related measures, multiple comparisons were corrected with each structure treated as a family, at two-tailed $p = 0.05 / (4 \text{ regions} \times 2 \text{ DBSI metrics}) = 0.00625$. Effect size estimates were standardized β's with 95% confidence intervals (CIs) and partial R^2's. Models were checked for normality of residuals, homoscedasticity, and low multicollinearity (variance inflation factors were ≤ 2.56). As there were missing data following outlier removal, sample sizes varied and are reported in individual analyses.

2.4.3. Comparison between DBSI and RSI

Mean RSI restricted normalized isotropic (RSI-RNI) metrics in bilateral nucleus accumbens, caudate nucleus, and putamen were obtained from the ABCD Study® tabulated dataset (Hagler et al., 2019). The ABCD Study® segmented structures using FreeSurfer v5.3; the hypothalamus was not specifically segmented and voxel-wise RSI-RNI maps were not available. RSI reflects cellularity as an increase in the restricted isotropic (originating from intracellular water) diffusion signal, i.e., RSI-RNI (Rapuano et al., 2020, 2022). Associations between RSI-RNI and baseline or future change in obesity-related measures were evaluated using linear mixed-effects models, as in DBSI described in **section 2.4.2**. To further compare model performance, DBSI-RF and RSI-RNI from the nucleus accumbens, caudate nucleus, and putamen were each tested on classifying NW and OB participants using mixed-effects logistic regression, with the same fixed and random effect covariates in linear models. Receiver operating characteristic curves and areas-under-the-curve (AUCs) with 95% CIs were computed using the *pROC* package, and AUCs from DBSI-RF and RSI-RNI were compared using DeLong's test (Robin et al., 2011).

3. Results

3.1. Sample characteristics

Participant demographics, neuroimaging metrics, and obesity-related measures are described in **Table 1**. Qualitatively, the OW and/or OB groups compared to the NW group had more non-White participants, more advanced pubertal development, lower parental education, household income, and proportion of married parents, higher baseline obesity-related measures, and greater one and two-year gain in WC but decrease in BMI *z*-scores. Groups did not differ significantly in striatal or hypothalamic volumes; these volumes were thus not covaried in addition to ICV in analyses.

Variable	**Group** (total *n* = 601)			***p*-value**
	NW	**OW**	**OB**	
n	212 (35.3% of all)	187 (31.1% of all)	202 (33.6% of all)	N/A
Age (months)	121 ± 8	121 ± 7	120 ± 7	0.89
Sex				
Male	113 (53.3%)	98 (52.4%)	120 (59.4%)	0.31
Female	99 (46.7%)	89 (47.6%)	82 (40.6%)	
Race/ethnicity				
Asian	1 (0.5%)	1 (0.5%)	4 (2.0%)	< 0.001 ***
Black	16 (7.5%)	23 (12.3%)	27 (13.4%)	
Hispanic	25 (11.8%)	37 (19.8%)	54 (26.7%)	
White	156 (73.6%)	112 (59.9%)	99 (49.0%)	
Other	14 (6.6%)	14 (7.5%)	18 (8.9%)	
PDS category				
1	129 (60.8%)	76 (40.6%)	86 (42.6%)	< 0.001 ***
2	53 (25.0%)	49 (26.2%)	51 (25.2%)	
3+	30 (14.2%)	62 (33.2%)	65 (32.2%)	
Parental education				
No HS diploma	0 (0%)	1 (0.5%)	4 (2.0%)	< 0.001 **
HS diploma/ GED	7 (3.3%)	5 (2.7%)	20 (9.9%)	
Some college	14 (6.6%)	28 (15.0%)	42 (20.8%)	
Bachelor	97 (45.8%)	87 (46.5%)	84 (41.6%)	
Postgraduate	94 (44.3%)	66 (35.3%)	52 (25.7%)	
Household income				
< 50k	32 (15.1%)	45 (24.1%)	62 (30.7%)	< 0.001 ***
≥ 50k & < 100k	64 (30.2%)	74 (39.6%)	74 (36.6%)	
≥ 100k	116 (54.7%)	68 (36.4%)	66 (32.7%)	
Parental marriage				
Married	164 (77.4%)	128 (68.4%)	127 (62.9%)	0.005 **
Not married	48 (22.6%)	59 (31.6%)	75 (37.1%)	
Mean motion (mm)	1.23 ± 0.25	1.27 ± 0.31	1.27 ± 0.30	0.25
ICV (mm^3)	1539012 ± 128794	1569834 ± 151931	1559140 ± 144992	0.09
$V_{hypothalamus}$ (mm^3)	737 ± 90	740 ± 104	733 ± 108	0.77
$V_{nucleus\ accumbens}$ (mm^3)	1028 ± 204	1057 ± 225	1034 ± 204	0.36
$V_{caudate\ nucleus}$ (mm^3)	7902 ± 990	8038 ± 975	7853 ± 998	0.16
$V_{putamen}$ (mm^3)	10609 ± 1154	10691 ± 1162	10627 ± 1206	0.77
Obesity-related measures				
Baseline				
BMI (kg/m^2)	16.82 ± 1.39	20.92 ± 1.06	25.85 ± 3.41	< 0.001 ***
BMI percentile	48.51 ± 22.38	90.43 ± 2.90	97.63 ± 1.32	< 0.001 ***
BMI *z*-score	-0.06 ± 0.65	1.33 ± 0.17	2.05 ± 0.29	< 0.001 ***
WC (inch)	25.13 ± 2.27	29.16 ± 2.68	32.96 ± 4.10	< 0.001 ***
One-year				
BMI (kg/m^2)	17.61 ± 1.88	21.97 ± 2.24	27.16 ± 4.63	< 0.001 ***
BMI *z*-score	-0.01 ± 0.75	1.28 ± 0.47	1.98 ± 0.53	< 0.001 ***
WC (in)	25.93 ± 2.68	30.03 ± 2.82	34.89 ± 4.48	< 0.001 ***
Change (Δ) over one year				
ΔBMI (kg/m^2)	0.79 ± 1.29	1.05 ± 1.97	1.30 ± 3.57	0.12
ΔBMI *z*-score	0.04 ± 0.51	-0.05 ± 0.44	-0.08 ± 0.45	0.024 *
ΔWC (in)	0.80 ± 2.34	0.88 ± 2.66	1.94 ± 3.16	< 0.001 ***
Two-year				
BMI (kg/m^2)	18.43 ± 2.32	22.91 ± 2.48	28.11 ± 4.81	< 0.001 ***
BMI *z*-score	0.01 ± 0.86	1.28 ± 0.50	1.94 ± 0.54	< 0.001 ***
WC (in)	27.12 ± 3.01	31.34 ± 3.27	36.02 ± 4.98	< 0.001 ***
Change (Δ) over two years				
ΔBMI (kg/m^2)	1.62 ± 1.83	1.98 ± 2.27	2.25 ± 3.85	0.07
ΔBMI *z*-score	0.07 ± 0.65	-0.05 ± 0.48	-0.11 ± 0.48	0.002 **
ΔWC (in)	1.99 ± 2.72	2.18 ± 3.01	3.06 ± 3.72	0.001 **

Table 1. Participant demographics, brain volumes, and obesity-related measures. Statistics are shown as mean ± standard deviation for continuous variables and count (frequency) for categorical data. Variables were assessed at baseline unless otherwise noted. Comparisons were performed using one-way analysis of variance or chi-squared tests as appropriate. The "Other" category under race/ethnicity included participants who were parent/caregiver-identified as American Indian, Alaskan Native, Native Hawaiian, other Pacific Islander, mixed, or otherwise not listed. Abbreviations: NW, children with normal-weight; OW, with overweight; OB, with obesity; PDS, pubertal development stage; HS, high school; GED, General Educational Development; ICV, intracranial volume; V, volume; BMI, body mass index; WC, waist circumference. *, $p \leq 0.05$; **, $p \leq 0.01$; ***, $p \leq 0.001$.

3.2. Comparison of white matter DBSI metrics across groups

TBSS ANOVAs indicated significant main effects of weight group for both DBSI-FF and RF. Follow-up TBSS *t*-tests showed that relative to NW, both OW and OB participants had significantly lower DBSI-FF (reflecting lower axonal/dendritic density) and greater DBSI-RF (reflecting elevated cellularity) in widespread white matter tracts (all FWE-corrected $p \leq 0.05$). Qualitatively, group differences in both DBSI-FF and RF appeared more widespread throughout white matter tracts in the OB vs. NW comparisons than in OW vs. NW comparisons (**Fig. 1**); nonetheless, white matter voxel-wise DBSI-FF and RF were not significantly different between OB and OW groups (FWE-corrected $p >$ 0.054). Consistent with voxel-wise comparisons, relative to NW, both OW and OB groups had lower white matter average DBSI-FF (OW vs. NW, $\beta = -0.39$, 95% CI: -0.60 to -0.18, $p < 0.001$; OB vs. NW, $\beta = -0.33$, 95% CI: -0.54 to -0.11, $p = 0.003$) and greater DBSI-RF (OW vs. NW, $\beta = 0.50$, 95% CI: 0.30 to 0.70, $p < 0.001$; OB vs. NW, $\beta = 0.36$, 95% CI: 0.16 to 0.56, $p < 0.001$), but these differences were not significant between OW and OB (p's = 0.65 and 0.14 for DBSI-FF and RF comparisons).

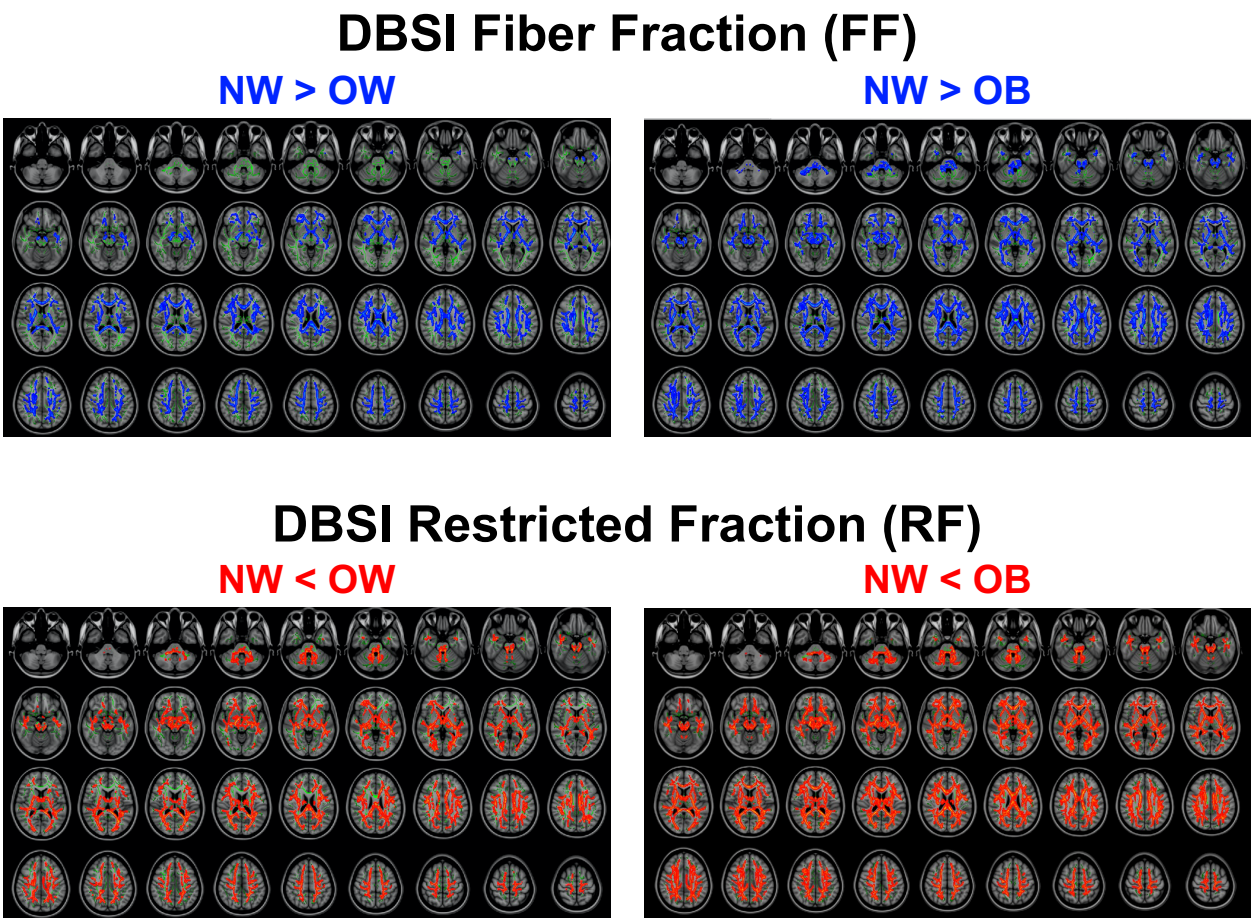

Fig. 1. Voxel-wise comparisons of white matter DBSI metrics amongst unrelated children with normal-weight (NW; n = 202), overweight (OW, n = 180) and obesity (OB; n = 191). In each panel, axial images are shown from inferior (top left) to superior (bottom right). In *green*: white matter skeleton; in *blue, light blue*: NW > OB/OW at family-wise error (FWE) rate-corrected $p \leq 0.05$ and 0.01; in *red, yellow*: NW < OB/OW at FWE-corrected $p \leq 0.05$ and 0.01. Comparisons were adjusted for age, sex, race/ethnicity, parental education, household income, parental marital status, pubertal development stage, mean head motion, and intracranial volume. DBSI, diffusion basis spectrum imaging.

3.3. Associations between striatal and hypothalamic DBSI metrics and obesity-related measures

3.3.1. Baseline

Greater BMI at baseline was significantly associated with greater DBSI-RF in the hypothalamus (β = 0.11, 95% CI: 0.04 to 0.19, partial R^2 = 0.014, p = 0.005), nucleus accumbens (β = 0.30, 95% CI: 0.22 to 0.39, partial R^2 = 0.096, p < 0.001), caudate nucleus (β = 0.18, 95% CI: 0.08 to 0.27, partial R^2 = 0.034, p < 0.001), and the putamen (β = 0.14, 95% CI: 0.06 to 0.22, partial R^2 = 0.021, p = 0.001) (**Fig. 2A**). These results were consistent with WC and BMI z-scores as obesity-related measures. Further,

350 greater baseline BMI *z*-scores were significantly related to lower DBSI-FF in the hypothalamus (β = -
351 0.12, 95% CI: -0.20 to -0.05, partial R^2 = 0.016, p = 0.002) (**Fig. 2B**). Similar associations, at nominal but
352 not multiple comparison-adjusted significance, were seen between lower DBSI-FF in the hypothalamus
353 and WC (β = -0.08, p = 0.038) and BMI (β = -0.09, p = 0.024); in the nucleus accumbens and WC (β = -
354 0.10, p = 0.009); and in the putamen and BMI (β = -0.08, p = 0.048) and BMI *z*-scores (β = -0.08, p =
355 0.048). Detailed statistics for all models are reported in **Supplementary Table 2**. Follow-up analyses
356 revealed no DBSI metric by hemisphere interaction in relating to baseline obesity-related measures (i.e.,
357 no laterality effect; p's ≥ 0.30).

358 Beyond DBSI metrics, variables that were associated with greater obesity-related measures at
359 baseline included older age, lower parental education, and more advanced pubertal stage. As we did not
360 specifically power or hypothesize for demographics-related effects, these findings are exploratory and are
361 noted in **Supplementary Table 3**. In total, our linear-mixed effects models explained 18-25% of the
362 variance in baseline obesity-related measures.

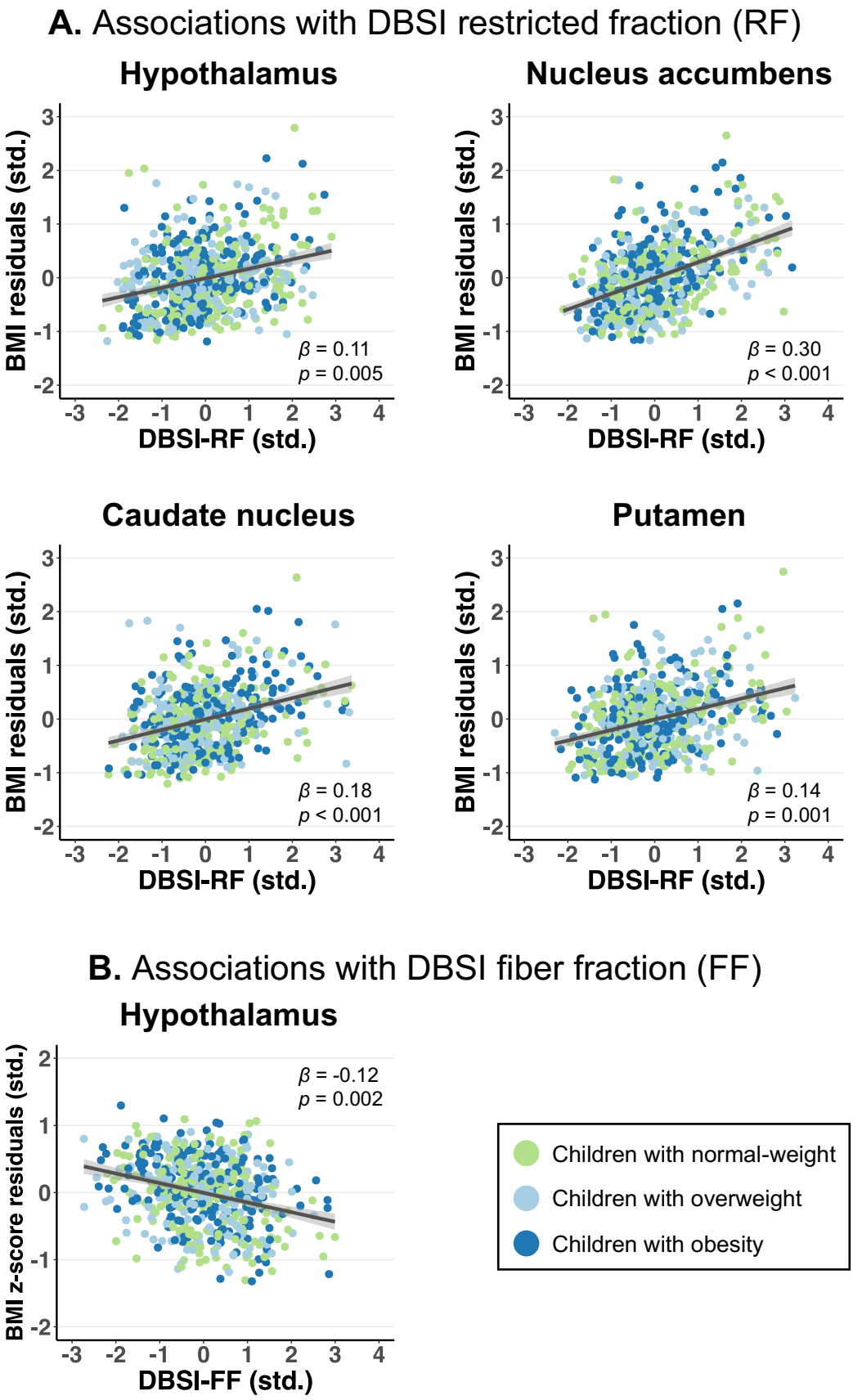
A. Associations with DBSI restricted fraction (RF)
Hypothalamus
Nucleus accumbens
Caudate nucleus
Putamen
BMI residuals (std.)
DBSI-RF (std.)
β = 0.11
p = 0.005
β = 0.30
p < 0.001
β = 0.18
p < 0.001
β = 0.14
p = 0.001
B. Associations with DBSI fiber fraction (FF)
Hypothalamus
BMI z-score residuals (std.)
DBSI-FF (std.)
β = -0.12
p = 0.002
Children with normal-weight
Children with overweight
Children with obesity

363

Fig. 2. Significant associations **(A)** between baseline body mass index (BMI) and DBSI-RF in the hypothalamus and striatum and **(B)** between baseline BMI *z*-scores and DBSI-FF in the hypothalamus in children. BMI or BMI *z*-score residuals (adjusted for age, sex, race/ethnicity, parental education, household income, parental marital status, pubertal development stage, mean head motion, intracranial volume, and family nested by site) and DBSI metrics were standardized (std.). Standardized β regression coefficients were reported with 95% confidence intervals (shaded). DBSI, diffusion basis spectrum imaging.

3.3.2. One and two-year change

Greater DBSI-RF in the hypothalamus at baseline, at nominal significance not surviving multiple comparison correction, predicted greater gain in WC over two years, accounting for baseline WC (β = 0.09, 95% CI: 0.01 to 0.18, partial R^2 = 0.008, p = 0.035; **Supplementary Fig. 4**). However, such effect was not seen at one-year follow-up, or with changes in BMI or BMI *z*-scores as obesity-related measures (*p*'s = 0.79 and 0.52). Other one or two-year changes in obesity-related measures were not associated with baseline DBSI metrics (**Supplementary Tables 4** and **5**).

3.4. Associations between striatal RSI-RNI and obesity-related measures

3.4.1. Baseline

Consistent with a previous study using ABCD Study® baseline data (n = 5,366; Rapuano et al., 2020), greater baseline BMI was associated with higher RSI-RNI in the nucleus accumbens (β = 0.36, 95% CI: 0.27 to 0.44, partial R^2 = 0.125, p < 0.001), caudate nucleus (β = 0.15, 95% CI: 0.07 to 0.23, partial R^2 = 0.025, p < 0.001), and putamen (β = 0.17, 95% CI: 0.09 to 0.26, partial R^2 = 0.030, p < 0.001) in the current, smaller sample. Results were similar with WC and BMI *z*-scores. Detailed statistics for all linear mixed-effects models are reported in **Supplementary Table 6**.

3.4.2. One and two-year change

Greater baseline RSI-RNI in the nucleus accumbens and caudate nucleus were respectively associated, not surviving multiple comparison correction, with one-year gain in WC, accounting for baseline levels (nucleus accumbens: β = 0.10, 95% CI: 0.00 to 0.20, partial R^2 = 0.008, p = 0.042; caudate nucleus: β = 0.11, 95% CI: 0.02 to 0.19, partial R^2 = 0.011, p = 0.017; **Supplementary Fig. 5**). These

associations were not seen at two-year follow-up or with changes in BMI or BMI *z*-scores (**Supplementary Tables 7** and **8**).

3.5. Comparison between DBSI and RSI on classifying NW and OB groups

Striatal DBSI and RSI metrics reflective of neuroinflammation-associated cellularity and cellular density, i.e., DBSI-RF and RSI-RNI, showed similar sensitivity and specificity in classifying NW and OB children (p's ≥ 0.13; **Fig. 3**). Across the striatum, DBSI-RF was positively and strongly correlated with RSI-RNI (r's ≥ 0.60, p's ≤ 0.001; **Supplementary Fig. 6**).

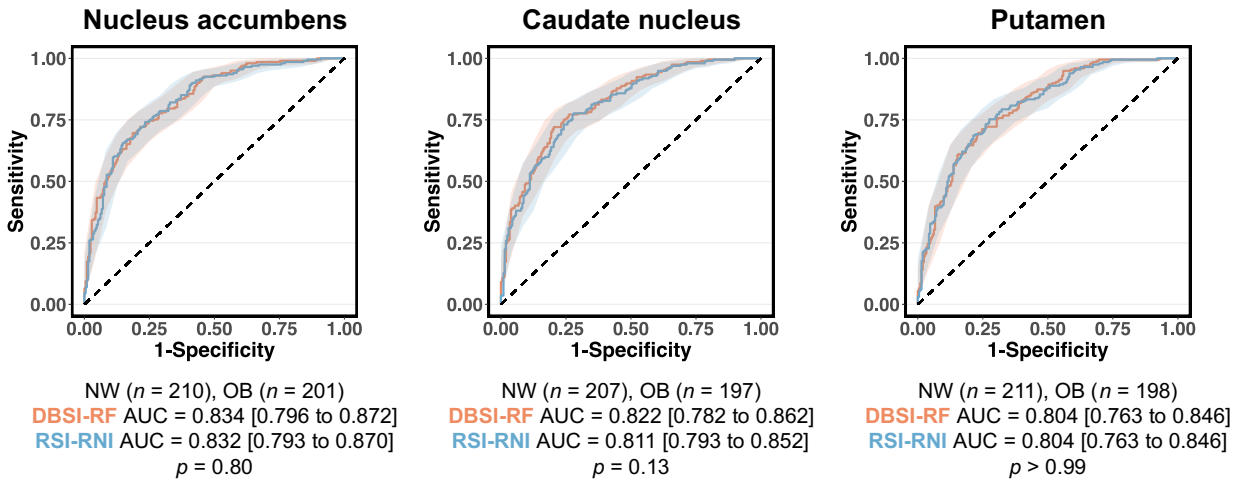

Fig. 3. Receiver operating characteristic curves comparing striatal DBSI restricted fraction (RF) and RSI restricted normalized isotropic (RNI) performance in classifying children with normal-weight (NW) and obesity (OB). AUC, area-under-the-curve; DBSI, diffusion basis spectrum imaging; RSI, restriction spectrum imaging.

4. Discussion

4.1. Overview

Here we present both novel findings and support for the reproducibility of previous neuroimaging studies that observed microstructural alterations suggestive of neuroinflammation in key feeding and reward-related brain regions in childhood obesity. First, we demonstrate that elevated DBSI-assessed cellularity, i.e., putative inflammatory marker, in the striatum relates to higher WC, BMI, and BMI *z*-scores in 601 children aged 9 to 11 years from the ABCD Study®, reproducing observations made by Rapuano et al., (2020) that used another diffusion-based RSI model in the same dataset. Quantitatively,

DBSI-RF and RSI-RNI were associated with obesity-related measures in similar magnitudes, and the two methods exhibited comparable performance in classifying NW vs. OB children. Such convergence of findings underpins the sensitivity and utility of diffusion MRI-based techniques in characterizing brain microstructural alterations in obesity.

Second, we observed associations between obesity and increased purported cellularity consistent with neuroinflammation in brain white matter tracts and hypothalamus, which were not assessed by Rapuano et al., (2020). Our results in the hypothalamus align with reports of putative gliosis in this region, assessed by quantitative T2 MRI, in both childhood and adult obesity (Schur et al., 2015; Sewaybricker et al., 2019; Sewaybricker, Kee, et al., 2021; Sewaybricker, Melhorn, et al., 2021; Thaler et al., 2012). Here, our findings add diffusion MRI-derived evidence of obesity-related putative neuroinflammation in the hypothalamus in children. Furthermore, to our knowledge, our study is the first to investigate and report overweight and obesity-associated white matter microstructural alterations in children, in line with our earlier studies of DBSI-assessed putative white matter neuroinflammation in adults (Samara et al., 2020). Collectively, our findings and those previously reported suggest that young children manifest obesity-related differences in brain microstructure that are consistent with neuroinflammation seen in animal and post-mortem human brain studies (Baufeld et al., 2016; Buckman et al., 2013; De Souza et al., 2005; Décarie-Spain et al., 2018; Schur et al., 2015; Valdearcos et al., 2017). Such brain differences may affect current and future susceptibility for weight gain and its comorbidities including cognitive impairment, type 2 diabetes, and late-life dementia (Liang et al., 2015; Simmonds et al., 2016; Tait et al., 2022).

4.2. Links between obesity, neuroinflammation, and brain function

The highly vascularized hypothalamus responds to feeding-related hormones, neuronal signals, and nutrients derived from the bloodstream (Velloso & Schwartz, 2011). As a “metabolic sensor”, the hypothalamus is vulnerable to overfeeding and obesity-related elevations in peripheral pro-inflammatory molecules including cytokines and saturated fatty acids (Jais & Brüning, 2017). Overfeeding also causes the blood-brain barrier to break down, further enabling inflammatory factors to infiltrate brain tissue

439 (Guillemot-Legris et al., 2016; Guillemot-Legris & Muccioli, 2017; Stranahan et al., 2016). Our finding
440 that DBSI-assessed cellularity (DBSI-RF) in the hypothalamus is greater in childhood obesity is
441 consistent with the neuroinflammatory phenotype encompassing the recruitment, proliferation, and
442 activation of astrocytes and microglia (i.e., reactive gliosis) seen in this brain region in rodents fed with
443 high-fat diets (Buckman et al., 2013; De Souza et al., 2005). While such immune response may initially
444 be neuroprotective, chronic gliosis leads to dysregulated neuroinflammatory processes that disrupt
445 hypothalamic metabolic regulation and contribute to overfeeding, leptin and insulin-resistance, and
446 development of obesity (Gómez-Apo et al., 2021; Sochocka et al., 2017; Valdearcos et al., 2017).
447 Persistent neuroinflammation could also cause axonal damage and loss (Frischer et al., 2009; Kempuraj et
448 al., 2016), which may explain our observed association between obesity and lower DBSI-assessed
449 axonal/dendritic density (DBSI-FF).

450 The striatum plays a key role in reward processing and appetitive behavior (Stice et al., 2011).
451 Striatal activity, primarily dopamine neurotransmission, is influenced by homeostatic signals from the
452 hypothalamus and by circulating feeding-related hormones, both acting on receptors on midbrain
453 dopaminergic cells (Abizaid et al., 2006; Figlewicz, 2016; Hommel et al., 2006; King et al., 2011).
454 Altered dopamine neurotransmission has been noted in obesity (Geiger et al., 2009; Wang et al., 2001;
455 Wu et al., 2017). Beyond the hypothalamus, neuroinflammation in the striatum may further contribute to
456 obesogenic behavior. Indeed, our observation of heightened DBSI-assessed cellularity across the striatum
457 in childhood obesity matches the microstructural changes characteristic of diet-induced reactive gliosis in
458 the nucleus accumbens in rodents (Décarie-Spain et al., 2018; Molina et al., 2020). Taken together, MRI-
459 based assessments of hypothalamic and striatal microstructure by us and others consistently suggest
460 putative neuroinflammation in these regions in childhood obesity, in agreement with studies in rodent
461 models and human adults.

462 Longitudinally, greater DBSI-assessed cellularity in the hypothalamus weakly predicted two-year
463 gain in WC, aligning with a recent T2 MRI-based report of putative hypothalamic gliosis being associated
464 with weight gain in children (Sewaybricker, Kee, et al., 2021). Further, greater RSI-RNI in the nucleus

accumbens and caudate nucleus were linked to one-year WC gain, reproducing findings in Rapuano et al., (2020). However, these findings were at nominal but not multiple comparison-corrected significance, and did not generalize across different obesity-related measures or MRI techniques. As our sample size was not intended to power for the weaker longitudinal effects observed in Rapuano et al., (2020), these findings require confirmation in larger studies involving more longitudinal observations as the ABCD Study® continues to release data. Nonetheless, given evidence that striatal neuroinflammation causally contribute to overfeeding in rodents (Décarie-Spain et al., 2018), plus emerging reports that putative nucleus accumbens cellularity may mediate the relationships between eating behavior and obesity in both adults and children (Rapuano et al., 2022; Samara et al., 2021), chronic neuroinflammation should be evaluated as a potential contributing factor to obesity maintenance.

4.3. Brain microstructure in childhood vs. adult obesity

Overall, the pattern of our results in children agrees with DBSI-assessed microstructural alterations seen in adult obesity (Ly et al., 2021; Samara et al., 2020, 2021). Obesity-associated decrease in apparent axonal/dendritic density and increase in cellularity have been observed in white matter in both adults and children. However, the pattern of results in the striatum differs by age. For example, greater putative cellularity in the nucleus accumbens is associated with higher BMI and related metrics in children, but such effect is absent in adults (Samara et al., 2021). Interestingly, it has been noted that in adults, higher BMI is associated with smaller nucleus accumbens volumes (Dekkers et al., 2019; García-García et al., 2020), whereas in children, such association is reversed (García-García et al., 2020; Rapuano et al., 2017) or absent, as is in the current study and another analysis of the ABCD Study® data (Adise et al., 2021). It is possible that as early reactive responses to obesity, striatal cellularity and gliosis would manifest as microstructural but not volumetric alterations in children, while chronic neuroinflammation would over time contribute to vasogenic edema and atrophy seen in adults (Dorrance et al., 2014; Sochocka et al., 2017), as in multiple sclerosis (Kamholz & Garbern, 2005). Furthermore, as executive control regions such as the prefrontal cortex mature later relative to the striatum (Spear, 2000), striatal disruptions may lead to a more dysregulated reward system that influences obesogenic behavior

more strongly in children than in adults. As the ABCD Study® collects biennial neuroimaging scans in the same participants from childhood through adulthood using harmonized MRI sequences, future research should capitalize on this longitudinal dataset to delineate obesity-related brain microstructural changes over development.

4.4. Comparison between DBSI and RSI findings

Although DBSI and RSI differ in their modeling of brain microstructure, their measures of restricted water diffusion have been interpreted similarly such that the isotropic intracellular water fraction (DBSI-RF and RSI-RNI) is thought to ultimately reflect the degree of neuroinflammation-related immune cell infiltration or tissue cellularity (Cross & Song, 2017; Rapuano et al., 2020, 2022; Wang et al., 2011, 2015). Indeed, in our study, DBSI and RSI-assessed striatal cellularity related similarly to obesity-related measures and strongly with each other, and classified obesity status with comparable performance. A true head-to-head comparison of the microstructural properties reflected by DBSI-RF and RSI-RNI would however warrant a controlled phantom or immunohistological gold standard. In general, the agreeing findings from DBSI and RSI highlight that diffusion MRI-based techniques are sensitive to characterizing obesity-associated microstructural alterations in children, adding a novel neuroimaging tool that assesses putative neuroinflammation *in vivo*.

4.5. Limitations

Limitations and future directions include, first, the lack of longitudinal timepoints besides one and two-year follow-ups. It is possible that obesity-related neuroinflammation affects clinical and behavioral outcomes on a timescale larger than two years. Second, as the ABCD Study® does not record obesity duration, we could not assess when and to what extent brain microstructural changes occur relative to obesity onset. Further research tracking children moving from normal-weight to obesity would be useful. Third, as we focused on assessing associations between brain microstructure and obesity-related measures, factors such as sex and socioeconomic status (SES) that likely impact child development and complicate said associations, though controlled for in analyses, were not tested. In terms of sex, girls have greater fat mass and more concentrated trunk adiposity than boys, even at similar BMIs

517 (Wisniewski & Chernausek, 2009). Further, though obesity is associated with elevated serum leptin levels
518 in both sexes, such effect is stronger in girls, who also demonstrate increases in leptin during puberty as
519 opposed to decreases in boys (Falorni et al., 1997). In terms of SES, socioeconomic adversity is a known
520 risk factor for childhood obesity (Hemmingsson, 2018; Vazquez & Cubbin, 2020), with physical
521 inactivity, unhealthy diet, and stress as proposed mediating mechanisms (Caprio et al., 2008;
522 Gebremariam et al., 2017; Hemmingsson, 2018; Mekonnen et al., 2020). Studies have also noted that girls
523 from disadvantaged neighborhoods are more susceptible to obesity compared to boys (Kranjac et al.,
524 2021), and that girls and boys experience differential dietary influences and weight expectations from
525 parents and peers (Caprio et al., 2008; Shah et al., 2020). Regarding brain microstructure, recent analyses
526 using the ABCD Study® data have shown that girls demonstrate greater RSI-assessed cell and neurite
527 density in white matter compared to boys (Lawrence et al., 2022), and lower SES interacts with greater
528 BMI in relating to putative white matter neuroinflammation and smaller brain volumes (Adise et al.,
529 2022; Dennis et al., 2022; Li et al., 2023). Collectively, these results suggest that there exist complex
530 associations between sex, sociocultural forces, and brain microstructure, and future research should adopt
531 an integrative framework to investigate how they may individually and interactively shape obesity
532 development. On a related note, we emphasize growing concerns that current practices of MRI acquisition
533 and quality control may inadvertently exclude participants in less accessible rural areas, from lower SES
534 families, and of racial/ethnic minorities (Ricard et al., 2023). The exclusion of neuroimaging data with
535 excessive head motion, in particular, poses a challenge in obesity research, as greater BMI is causally and
536 genetically linked to increased motion (Beyer et al., 2020). It is possible that our findings may not
537 generalize to children of all sociodemographic backgrounds, and confirmation in large samples of
538 marginalized populations is needed.

539 Finally, we note the limited interpretability of diffusion MRI-derived microstructural metrics.
540 While DBSI assessments have been histopathologically validated as neuroinflammation-sensitive in
541 inflammatory neurological diseases including human and rodent models of multiple sclerosis (Chiang et
542 al., 2014; Wang et al., 2011, 2015), and rodent optic neuritis (Lin et al., 2017; Yang et al., 2021),

validation remains ongoing for obesity. Although the cellularity and axonal density effects inferred from DBSI-modeled water diffusivity agree with the neuroinflammatory phenotype seen in animal models and human post-mortem brain of obesity (Baufeld et al., 2016; Buckman et al., 2013; De Souza et al., 2005; Décarie-Spain et al., 2018; Schur et al., 2015; Valdearcos et al., 2017), we recognize that DBSI, as any MRI technique, is an indirect marker of brain microstructure and could reflect neural development that otherwise do not involve neuroinflammation (Palmer et al., 2022). On a related note, it is challenging to determine whether feeding-related regions such as the hypothalamus and striatum are the only ones involved in obesity-related neuroinflammation, since a true control region in which this phenomenon is definitively absent has not been identified. Such limitation invites future research to evaluate microstructure throughout gray matter as well as study potential interactions between gray and white matter alterations in obesity. The confidence in the validity of MRI-based assessments of obesity-related neuroinflammation could be explored with rodent models and/or human studies using positron emission tomography methods for measuring neuroinflammatory indicators (e.g., astrocyte and microglia activation).

5. Conclusions

With DBSI, we observed microstructural alterations in white matter, hypothalamus, and striatum in children with overweight and obesity. Agreement between DBSI and RSI suggested that diffusion MRI is a sensitive and useful tool for assessing obesity-related putative cellularity in children. Given that childhood and adolescence involve substantial brain development, further longitudinal work is warranted to elucidate how early changes in brain microstructure may contribute to obesity and its comorbidities in the long run.

Funding: This work was supported by the National Institutes of Health (NIH) grants R01DK085575 (Hershey), T32DA007261-29 (Samara, Ray, Eisenstein), 1RF1AG072637-01 (Raji), KL2TR000450 in partial form of Washington University Institute of Clinical and Translational Sciences Multidisciplinary Clinical Research Career Development Program to (Ray, Raji), P30DK020579 in partial form of Washington University Diabetes Research Center Pilot & Feasibility Award to (Eisenstein); the Washington University Neuroimaging Laboratory Research Center Innovation Funds (Eisenstein), the Radiological Society of North America Research Scholar Grant (Raji), the Mallinckrodt Institute of Radiology Pilot Award (Eisenstein) and Summer Research Program (Li), the Society for Neuroscience Trainee Professional Development Award (Li), the Washington University Summer Undergraduate Research Award (Li), and Washington University McDonnell Center for Systems Neuroscience. The ABCD Study® is supported by the NIH and federal partners (grants U01DA041048, U01DA050989, U01DA051016, U01DA041022, U01DA051018, U01DA051037, U01DA050987, U01DA041174, U01DA041106, U01DA041117, U01DA041028, U01DA041134, U01DA050988, U01DA051039, U01DA041156, U01DA041025, U01DA041120, U01DA051038, U01DA041148, U01DA041093, U01DA041089, U24DA041123, and U24DA041147). A full list of supporters is available at https://abcdstudy.org/federal-partners.html. The funders had no role in study design, data collection and analysis, preparation of the manuscript, or decision to publish. The content is solely the responsibility of the authors and does not necessarily represent the official views of the National Institutes of Health or other funders.

Conflict of interest disclosures: Unrelated to this study, Dr. Cyrus A. Raji consults to Brainreader, Neurevolution, Voxelwise, and the Pacific Neuroscience Foundation. Other authors have no conflict of interest to disclose.

Author contributions (CRediT): Zhaolong Li, BA: Conceptualization, Data curation, Formal analysis, Methodology, Software, Visualization, Writing – original draft, Writing – review & editing; **Amjad Samara, MD:** Conceptualization, Data curation, Formal analysis, Software, Writing – Review & Editing; **Mary Katherine Ray, PhD:** Conceptualization, Formal analysis, Writing – original draft, Writing – Review & Editing; **Jerrel Rutlin, BS:** Data curation, Software; **Cyrus A. Raji, MD, PhD:** Writing – review & editing; **Joshua S. Shimony, MD, PhD:** Writing – review & editing; **Peng Sun, PhD:** Methodology, Writing – review & editing; **Sheng-Kwei Song, PhD:** Methodology, Writing – review & editing; **Tamara Hershey, PhD:** Conceptualization, Methodology, Supervision, Writing – review & editing; **Sarah A. Eisenstein, PhD:** Conceptualization, Formal analysis, Methodology, Software, Supervision, Validation, Writing – original draft, Writing – review & editing

Acknowledgements: The authors wish to thank Richard Ni, Jonathan Koller, and Heather Lugar for their assistance with neuroimaging analyses in this study.

Data availability statement: The ABCD Study® data are publicly available through the National Institute of Mental Health Data Archive (https://nda.nih.gov/abcd). The ABCD Study® data used in this report came from the ABCD Study® Data Release 2.0.1 (DOI: DOI 10.15154/1506087, July 2019) and 4.0 (DOI: 10.15154/1523041, October 2021). The p-code of script used to generate DBSI maps in this study are available upon request, and the developers of DBSI are in the process of publishing an open-source version of the scripts.

608 **References**

609 Abizaid, A., Liu, Z.-W., Andrews, Z. B., Shanabrough, M., Borok, E., Elsworth, J. D., Roth, R. H.,
610 Sleeman, M. W., Picciotto, M. R., Tschöp, M. H., Gao, X.-B., & Horvath, T. L. (2006). Ghrelin
611 modulates the activity and synaptic input organization of midbrain dopamine neurons while
612 promoting appetite. *The Journal of Clinical Investigation*, *116*(12), 3229–3239.
613 https://doi.org/10.1172/JCI29867

614 Adise, S., Allgaier, N., Laurent, J., Hahn, S., Chaarani, B., Owens, M., Yuan, D., Nyugen, P., Mackey, S.,
615 Potter, A., & Garavan, H. P. (2021). Multimodal brain predictors of current weight and weight gain
616 in children enrolled in the ABCD study ®. *Developmental Cognitive Neuroscience*, *49*, 100948.
617 https://doi.org/10.1016/j.dcn.2021.100948

618 Adise, S., Marshall, A. T., Kan, E., Gonzalez, M. R., & Sowell, E. R. (2022). Relating neighborhood
619 deprivation to childhood obesity in the ABCD study: Evidence for theories of neuroinflammation
620 and neuronal stress. *Health Psychology : Official Journal of the Division of Health Psychology,*
621 *American Psychological Association*. https://doi.org/10.1037/hea0001250

622 Barch, D. M., Albaugh, M. D., Avenevoli, S., Chang, L., Clark, D. B., Glantz, M. D., Hudziak, J. J.,
623 Jernigan, T. L., Tapert, S. F., Yurgelun-Todd, D., Alia-Klein, N., Potter, A. S., Paulus, M. P.,
624 Prouty, D., Zucker, R. A., & Sher, K. J. (2018). Demographic, physical and mental health
625 assessments in the adolescent brain and cognitive development study: Rationale and description.
626 *Developmental Cognitive Neuroscience*, *32*, 55–66.
627 https://doi.org/https://doi.org/10.1016/j.dcn.2017.10.010

628 Bates, D., Mächler, M., Bolker, B., & Walker, S. (2015). Fitting Linear Mixed-Effects Models Using
629 lme4. *Journal of Statistical Software; Vol 1, Issue 1 (2015)* . https://www.jstatsoft.org/v067/i01

630 Baufeld, C., Osterloh, A., Prokop, S., Miller, K. R., & Heppner, F. L. (2016). High-fat diet-induced brain
631 region-specific phenotypic spectrum of CNS resident microglia. *Acta Neuropathologica*, *132*(3),
632 361–375. https://doi.org/10.1007/s00401-016-1595-4

633 Beilharz, J. E., Maniam, J., & Morris, M. J. (2016). Short-term exposure to a diet high in fat and sugar, or
634 liquid sugar, selectively impairs hippocampal-dependent memory, with differential impacts on
635 inflammation. *Behavioural Brain Research*, *306*, 1–7.
636 https://doi.org/https://doi.org/10.1016/j.bbr.2016.03.018

637 Beyer, F., Prehn, K., Wüsten, K. A., Villringer, A., Ordemann, J., Flöel, A., & Witte, A. V. (2020).
638 Weight loss reduces head motion: Revisiting a major confound in neuroimaging. *Human Brain*
639 *Mapping*, *41*(9), 2490–2494. https://doi.org/10.1002/hbm.24959

640 Biener, A. I., Cawley, J., & Meyerhoefer, C. (2020). The medical care costs of obesity and severe obesity
641 in youth: An instrumental variables approach. *Health Economics*, *29*(5), 624–639.
642 https://doi.org/https://doi.org/10.1002/hec.4007

643 Billot, B., Bocchetta, M., Todd, E., Dalca, A. V., Rohrer, J. D., & Iglesias, J. E. (2020). Automated
644 segmentation of the hypothalamus and associated subunits in brain MRI. *NeuroImage*, *223*, 117287.
645 https://doi.org/10.1016/j.neuroimage.2020.117287

646 Birdsill, A. C., Oleson, S., Kaur, S., Pasha, E., Ireton, A., Tanaka, H., & Haley, A. (2017). Abdominal
647 obesity and white matter microstructure in midlife. *Human Brain Mapping*, *38*(7), 3337–3344.
648 https://doi.org/10.1002/hbm.23576

649 Buckman, L. B., Thompson, M. M., Moreno, H. N., & Ellacott, K. L. J. (2013). Regional astrogliosis in
650 the mouse hypothalamus in response to obesity. *Journal of Comparative Neurology*, *521*(6), 1322–

1333. https://doi.org/https://doi.org/10.1002/cne.23233

Caprio, S., Daniels, S. R., Drewnowski, A., Kaufman, F. R., Palinkas, L. A., Rosenbloom, A. L., & Schwimmer, J. B. (2008). Influence of race, ethnicity, and culture on childhood obesity: implications for prevention and treatment: a consensus statement of Shaping America's Health and the Obesity Society. *Diabetes Care*, *31*(11), 2211–2221. https://doi.org/10.2337/dc08-9024

Carbine, K. A., Duraccio, K. M., Hedges-Muncy, A., Barnett, K. A., Kirwan, C. B., & Jensen, C. D. (2020). White matter integrity disparities between normal-weight and overweight/obese adolescents: an automated fiber quantification tractography study. *Brain Imaging and Behavior*, *14*(1), 308–319. https://doi.org/10.1007/s11682-019-00036-4

Casey, B. J., Cannonier, T., Conley, M. I., Cohen, A. O., Barch, D. M., Heitzeg, M. M., Soules, M. E., Teslovich, T., Dellarco, D. V, Garavan, H., Orr, C. A., Wager, T. D., Banich, M. T., Speer, N. K., Sutherland, M. T., Riedel, M. C., Dick, A. S., Bjork, J. M., Thomas, K. M., … Dale, A. M. (2018). The Adolescent Brain Cognitive Development (ABCD) study: Imaging acquisition across 21 sites. *Developmental Cognitive Neuroscience*, *32*, 43–54. https://doi.org/https://doi.org/10.1016/j.dcn.2018.03.001

Chiang, C. W., Wang, Y., Sun, P., Lin, T. H., Trinkaus, K., Cross, A. H., & Song, S. K. (2014). Quantifying white matter tract diffusion parameters in the presence of increased extra-fiber cellularity and vasogenic edema. *NeuroImage*, *101*, 310–319. https://doi.org/10.1016/j.neuroimage.2014.06.064

Cole, T. J., Faith, M. S., Pietrobelli, A., & Heo, M. (2005). What is the best measure of adiposity change in growing children: BMI, BMI %, BMI z-score or BMI centile? *European Journal of Clinical Nutrition*, *59*(3), 419–425. https://doi.org/10.1038/sj.ejcn.1602090

Cross, A. H., & Song, S. K. (2017). "A new imaging modality to non-invasively assess multiple sclerosis pathology." *Journal of Neuroimmunology*, *304*, 81–85. https://doi.org/10.1016/j.jneuroim.2016.10.002

Daoust, J., Schaffer, J., Zeighami, Y., Dagher, A., García-García, I., & Michaud, A. (2021). White matter integrity differences in obesity: A meta-analysis of diffusion tensor imaging studies. *Neuroscience and Biobehavioral Reviews*, *129*, 133–141. https://doi.org/10.1016/j.neubiorev.2021.07.020

De Souza, C. T., Araujo, E. P., Bordin, S., Ashimine, R., Zollner, R. L., Boschero, A. C., Saad, M. J. A., & Velloso, L. A. (2005). Consumption of a fat-rich diet activates a proinflammatory response and induces insulin resistance in the hypothalamus. *Endocrinology*, *146*(10), 4192–4199. https://doi.org/10.1210/en.2004-1520

Décarie-Spain, L., Sharma, S., Hryhorczuk, C., Issa-Garcia, V., Barker, P. A., Arbour, N., Alquier, T., & Fulton, S. (2018). Nucleus accumbens inflammation mediates anxiodepressive behavior and compulsive sucrose seeking elicited by saturated dietary fat. *Molecular Metabolism*, *10*, 1–13. https://doi.org/10.1016/j.molmet.2018.01.018

Dekkers, I. A., Jansen, P. R., & Lamb, H. J. (2019). Obesity, Brain Volume, and White Matter Microstructure at MRI: A Cross-sectional UK Biobank Study. *Radiology*, *291*(3), 763–771. https://doi.org/10.1148/radiol.2019181012

Dennis, E., Manza, P., & Volkow, N. D. (2022). Socioeconomic status, BMI, and brain development in children. *Translational Psychiatry*, *12*(1), 33. https://doi.org/10.1038/s41398-022-01779-3

Dorrance, A. M., Matin, N., & Pires, P. W. (2014). The effects of obesity on the cerebral vasculature. *Current Vascular Pharmacology*, *12*(3), 462–472.

https://doi.org/10.2174/1570161112666140423222411

Falorni, A., Bini, V., Molinari, D., Papi, F., Celi, F., Stefano, G. Di, Berioli, M. G., Bacosi, M. L., & Contessa, G. (1997). Leptin serum levels in normal weight and obese children and adolescents: relationship with age, sex, pubertal development, body mass index and insulin. *International Journal of Obesity*, *21*(10), 881–890. https://doi.org/10.1038/sj.ijo.0800485

Fernández-Andújar, M., Morales-García, E., & García-Casares, N. (2021). Obesity and Gray Matter Volume Assessed by Neuroimaging: A Systematic Review. *Brain Sciences*, *11*(8). https://doi.org/10.3390/brainsci11080999

Figlewicz, D. P. (2016). Expression of receptors for insulin and leptin in the ventral tegmental area/substantia nigra (VTA/SN) of the rat: Historical perspective. *Brain Research*, *1645*, 68–70. https://doi.org/https://doi.org/10.1016/j.brainres.2015.12.041

Frischer, J. M., Bramow, S., Dal-Bianco, A., Lucchinetti, C. F., Rauschka, H., Schmidbauer, M., Laursen, H., Sorensen, P. S., & Lassmann, H. (2009). The relation between inflammation and neurodegeneration in multiple sclerosis brains. *Brain*, *132*(5), 1175–1189. https://doi.org/10.1093/brain/awp070

Garavan, H., Bartsch, H., Conway, K., Decastro, A., Goldstein, R. Z., Heeringa, S., Jernigan, T., Potter, A., Thompson, W., & Zahs, D. (2018). Recruiting the ABCD sample: Design considerations and procedures. *Developmental Cognitive Neuroscience*, *32*, 16–22. https://doi.org/10.1016/j.dcn.2018.04.004

García-García, I., Morys, F., & Dagher, A. (2020). Nucleus accumbens volume is related to obesity measures in an age-dependent fashion. *Journal of Neuroendocrinology*, *32*(12), e12812. https://doi.org/10.1111/jne.12812

Gebremariam, M. K., Lien, N., Nianogo, R. A., & Arah, O. A. (2017). Mediators of socioeconomic differences in adiposity among youth: a systematic review. *Obesity Reviews : An Official Journal of the International Association for the Study of Obesity*, *18*(8), 880–898. https://doi.org/10.1111/obr.12547

Geiger, B. M., Haburcak, M., Avena, N. M., Moyer, M. C., Hoebel, B. G., & Pothos, E. N. (2009). Deficits of mesolimbic dopamine neurotransmission in rat dietary obesity. *Neuroscience*, *159*(4), 1193–1199. https://doi.org/https://doi.org/10.1016/j.neuroscience.2009.02.007

Gómez-Apo, E., Mondragón-Maya, A., Ferrari-Díaz, M., & Silva-Pereyra, J. (2021). Structural Brain Changes Associated with Overweight and Obesity. *Journal of Obesity*, *2021*, 6613385. https://doi.org/10.1155/2021/6613385

Gregor, M. F., & Hotamisligil, G. S. (2011). Inflammatory Mechanisms in Obesity. *Annual Review of Immunology*, *29*(1), 415–445. https://doi.org/10.1146/annurev-immunol-031210-101322

Guillemot-Legris, O., Masquelier, J., Everard, A., Cani, P. D., Alhouayek, M., & Muccioli, G. G. (2016). High-fat diet feeding differentially affects the development of inflammation in the central nervous system. *Journal of Neuroinflammation*, *13*(1), 206. https://doi.org/10.1186/s12974-016-0666-8

Guillemot-Legris, O., & Muccioli, G. G. (2017). Obesity-Induced Neuroinflammation: Beyond the Hypothalamus. In *Trends in Neurosciences* (Vol. 40, Issue 4, pp. 237–253). Elsevier Ltd. https://doi.org/10.1016/j.tins.2017.02.005

Hagler, D. J., Hatton, S., Cornejo, M. D., Makowski, C., Fair, D. A., Dick, A. S., Sutherland, M. T., Casey, B. J., Barch, D. M., Harms, M. P., Watts, R., Bjork, J. M., Garavan, H. P., Hilmer, L., Pung, C. J., Sicat, C. S., Kuperman, J., Bartsch, H., Xue, F., … Dale, A. M. (2019). Image processing and

analysis methods for the Adolescent Brain Cognitive Development Study. *NeuroImage*, *202*, 116091. https://doi.org/https://doi.org/10.1016/j.neuroimage.2019.116091

Hemmingsson, E. (2018). Early Childhood Obesity Risk Factors: Socioeconomic Adversity, Family Dysfunction, Offspring Distress, and Junk Food Self-Medication. *Current Obesity Reports*, *7*(2), 204–209. https://doi.org/10.1007/s13679-018-0310-2

Hommel, J. D., Trinko, R., Sears, R. M., Georgescu, D., Liu, Z.-W., Gao, X.-B., Thurmon, J. J., Marinelli, M., & DiLeone, R. J. (2006). Leptin Receptor Signaling in Midbrain Dopamine Neurons Regulates Feeding. *Neuron*, *51*(6), 801–810. https://doi.org/10.1016/j.neuron.2006.08.023

Jais, A., & Brüning, J. C. (2017). Hypothalamic inflammation in obesity and metabolic disease. *Journal of Clinical Investigation*, *127*(1), 24–32. https://doi.org/10.1172/JCI88878

Jernigan, T. L., Brown, S. A., & Dowling, G. J. (2018). The Adolescent Brain Cognitive Development Study. *Journal of Research on Adolescence : The Official Journal of the Society for Research on Adolescence*, *28*(1), 154–156. https://doi.org/10.1111/jora.12374

Jiang, F., Li, G., Ji, W., Zhang, Y., Wu, F., Hu, Y., Zhang, W., Manza, P., Tomasi, D., Volkow, N. D., Gao, X., Wang, G.-J., & Zhang, Y. (2023). Obesity is associated with decreased gray matter volume in children: a longitudinal study. *Cerebral Cortex*, *33*(7), 3674–3682. https://doi.org/10.1093/cercor/bhac300

Kamholz, J. A., & Garbern, J. Y. (2005). Neuronal cell injury precedes brain atrophy in multiple sclerosis. *Neurology*, *64*(1), 176 LP – 176. https://doi.org/10.1212/WNL.64.1.176

Kempuraj, D., Thangavel, R., Natteru, P. A., Selvakumar, G. P., Saeed, D., Zahoor, H., Zaheer, S., Iyer, S. S., & Zaheer, A. (2016). Neuroinflammation Induces Neurodegeneration. *Journal of Neurology, Neurosurgery and Spine*, *1*(1).

Killedar, A., Lung, T., Petrou, S., Teixeira-Pinto, A., Tan, E. J., & Hayes, A. (2020). Weight status and health-related quality of life during childhood and adolescence: effects of age and socioeconomic position. *International Journal of Obesity*, *44*(3), 637–645. https://doi.org/10.1038/s41366-020-0529-3

King, S. J., Isaacs, A. M., O'Farrell, E., & Abizaid, A. (2011). Motivation to obtain preferred foods is enhanced by ghrelin in the ventral tegmental area. *Hormones and Behavior*, *60*(5), 572–580. https://doi.org/https://doi.org/10.1016/j.yhbeh.2011.08.006

Kranjac, A. W., Boyd, C., Kimbro, R. T., Moffett, B. S., & Lopez, K. N. (2021). Neighborhoods matter; but for whom? Heterogeneity of neighborhood disadvantage on child obesity by sex. *Health & Place*, *68*, 102534. https://doi.org/https://doi.org/10.1016/j.healthplace.2021.102534

Kuczmarski, R. J., Ogden, C. L., Guo, S. S., Grummer-Strawn, L. M., Flegal, K. M., Mei, Z., Wei, R., Curtin, L. R., Roche, A. F., & Johnson, C. L. (2002). 2000 CDC Growth Charts for the United States: methods and development. *Vital and Health Statistics. Series 11, Data from the National Health Survey*, *246*, 1–190.

Kullmann, S, Schweizer, F., Veit, R., Fritsche, A., & Preissl, H. (2015). Compromised white matter integrity in obesity. *Obesity Reviews*, *16*(4), 273–281. https://doi.org/https://doi.org/10.1111/obr.12248

Kullmann, Stephanie, Callaghan, M. F., Heni, M., Weiskopf, N., Scheffler, K., Häring, H.-U., Fritsche, A., Veit, R., & Preissl, H. (2016). Specific white matter tissue microstructure changes associated with obesity. *NeuroImage*, *125*, 36–44. https://doi.org/https://doi.org/10.1016/j.neuroimage.2015.10.006

Lawrence, K. E., Abaryan, Z., Laltoo, E., Hernandez, L. M., Gandal, M. J., McCracken, J. T., & Thompson, P. M. (2022). White matter microstructure shows sex differences in late childhood: Evidence from 6797 children. *Human Brain Mapping*, *n/a*(n/a). https://doi.org/https://doi.org/10.1002/hbm.26079

Li, H., Nickerson, L. D., Nichols, T. E., & Gao, J.-H. (2017). Comparison of a non-stationary voxelation-corrected cluster-size test with TFCE for group-Level MRI inference. *Human Brain Mapping*, *38*(3), 1269–1280. https://doi.org/https://doi.org/10.1002/hbm.23453

Li, Y., Thompson, W. K., Reuter, C., Nillo, R., Jernigan, T., Dale, A., Sugrue, L. P., Brown, J., Dougherty, R. F., Rauschecker, A., Rudie, J., Barch, D. M., Calhoun, V., Hagler, D., Hatton, S., Tanabe, J., Marshall, A., Sher, K. J., Heeringa, S., … Brown, S. (2021). Rates of Incidental Findings in Brain Magnetic Resonance Imaging in Children. *JAMA Neurology*, *78*(5), 578–587. https://doi.org/10.1001/jamaneurol.2021.0306

Li, Z. A., Cai, Y., Taylor, R. L., Eisenstein, S. A., Barch, D. M., Marek, S., & Hershey, T. (2023). Associations between socioeconomic status and white matter microstructure in children: indirect effects via obesity and cognition. *MedRxiv*, 2023.02.09.23285150. https://doi.org/10.1101/2023.02.09.23285150

Liang, Y., Hou, D., Zhao, X., Wang, L., Hu, Y., Liu, J., Cheng, H., Yang, P., Shan, X., Yan, Y., Cruickshank, J. K., & Mi, J. (2015). Childhood obesity affects adult metabolic syndrome and diabetes. *Endocrine*, *50*(1), 87–92. https://doi.org/10.1007/s12020-015-0560-7

Lin, T.-H., Chiang, C.-W., Perez-Torres, C. J., Sun, P., Wallendorf, M., Schmidt, R. E., Cross, A. H., & Song, S.-K. (2017). Diffusion MRI quantifies early axonal loss in the presence of nerve swelling. *Journal of Neuroinflammation*, *14*(1), 78. https://doi.org/10.1186/s12974-017-0852-3

Ling, J., Merideth, F., Caprihan, A., Pena, A., Teshiba, T., & Mayer, A. R. (2012). Head injury or head motion? Assessment and quantification of motion artifacts in diffusion tensor imaging studies. *Human Brain Mapping*, *33*(1), 50–62. https://doi.org/10.1002/hbm.21192

Ly, M., Raji, C. A., Yu, G. Z., Wang, Q., Wang, Y., Schindler, S. E., An, H., Samara, A., Eisenstein, S. A., Hershey, T., Smith, G., Klein, S., Liu, J., Xiong, C., Ances, B. M., Morris, J. C., & Benzinger, T. L. S. (2021). Obesity and White Matter Neuroinflammation Related Edema in Alzheimer's Disease Dementia Biomarker Negative Cognitively Normal Individuals. *Journal of Alzheimer's Disease*, *79*, 1801–1811. https://doi.org/10.3233/JAD-201242

Mekonnen, T., Havdal, H. H., Lien, N., O'Halloran, S. A., Arah, O. A., Papadopoulou, E., & Gebremariam, M. K. (2020). Mediators of socioeconomic inequalities in dietary behaviours among youth: A systematic review. *Obesity Reviews*, *21*(7), e13016. https://doi.org/https://doi.org/10.1111/obr.13016

Molina, J., Joaquim, A., Bonamin, L. V., Martins, M. de F. M., Kirsten, T. B., Cardoso, C. V., Bernardi, M. M., & Bondan, E. F. (2020). Reduced astrocytic expression of GFAP in the offspring of female rats that received hypercaloric diet. *Nutritional Neuroscience*, *23*(6), 411–421. https://doi.org/10.1080/1028415X.2018.1512783

Neudorfer, C., Germann, J., Elias, G. J. B., Gramer, R., Boutet, A., & Lozano, A. M. (2020). A high-resolution in vivo magnetic resonance imaging atlas of the human hypothalamic region. *Scientific Data*, *7*(1), 305. https://doi.org/10.1038/s41597-020-00644-6

Palmer, C. E., Pecheva, D., Iversen, J. R., Hagler, D. J., Sugrue, L., Nedelec, P., Fan, C. C., Thompson, W. K., Jernigan, T. L., & Dale, A. M. (2022). Microstructural development from 9 to 14 years: Evidence from the ABCD Study. *Developmental Cognitive Neuroscience*, *53*, 101044.

824 https://doi.org/https://doi.org/10.1016/j.dcn.2021.101044

825 Patenaude, B., Smith, S. M., Kennedy, D. N., & Jenkinson, M. (2011). A Bayesian model of shape and
826 appearance for subcortical brain segmentation. *NeuroImage*, *56*(3), 907–922.
827 https://doi.org/https://doi.org/10.1016/j.neuroimage.2011.02.046

828 Pistell, P. J., Morrison, C. D., Gupta, S., Knight, A. G., Keller, J. N., Ingram, D. K., & Bruce-Keller, A. J.
829 (2010). Cognitive impairment following high fat diet consumption is associated with brain
830 inflammation. *Journal of Neuroimmunology*, *219*(1–2), 25–32.
831 https://doi.org/10.1016/j.jneuroim.2009.11.010

832 R Core Team. (2013). *R: A language and environment for statistical computing*. R Foundation for
833 Statistical Computing.

834 Raji, C. A., Ho, A. J., Parikshak, N. N., Becker, J. T., Lopez, O. L., Kuller, L. H., Hua, X., Leow, A. D.,
835 Toga, A. W., & Thompson, P. M. (2010). Brain structure and obesity. *Human Brain Mapping*,
836 *31*(3), 353–364. https://doi.org/https://doi.org/10.1002/hbm.20870

837 Rapuano, K. M., Berrian, N., Baskin-Sommers, A., Décarie-Spain, L., Sharma, S., Fulton, S., Casey, B.
838 J., & Watts, R. (2022). Longitudinal Evidence of a Vicious Cycle Between Nucleus Accumbens
839 Microstructure and Childhood Weight Gain. *Journal of Adolescent Health*.
840 https://doi.org/https://doi.org/10.1016/j.jadohealth.2022.01.002

841 Rapuano, K. M., Laurent, J. S., Hagler, D. J., Hatton, S. N., Thompson, W. K., Jernigan, T. L., Dale, A.
842 M., Casey, B. J., & Watts, R. (2020). Nucleus accumbens cytoarchitecture predicts weight gain in
843 children. *Proceedings of the National Academy of Sciences*, *117*(43), 26977–26984.
844 https://doi.org/10.1073/pnas.2007918117

845 Rapuano, K. M., Zieselman, A. L., Kelley, W. M., Sargent, J. D., Heatherton, T. F., & Gilbert-Diamond,
846 D. (2017). Genetic risk for obesity predicts nucleus accumbens size and responsivity to real-world
847 food cues. *Proceedings of the National Academy of Sciences*, *114*(1), 160 LP – 165.
848 https://doi.org/10.1073/pnas.1605548113

849 Ricard, J. A., Parker, T. C., Dhamala, E., Kwasa, J., Allsop, A., & Holmes, A. J. (2023). Confronting
850 racially exclusionary practices in the acquisition and analyses of neuroimaging data. *Nature*
851 *Neuroscience*, *26*(1), 4–11. https://doi.org/10.1038/s41593-022-01218-y

852 Robin, X., Turck, N., Hainard, A., Tiberti, N., Lisacek, F., Sanchez, J.-C., & Müller, M. (2011). pROC:
853 an open-source package for R and S+ to analyze and compare ROC curves. *BMC Bioinformatics*,
854 *12*(1), 77. https://doi.org/10.1186/1471-2105-12-77

855 Samara, A., Li, Z., Rutlin, J., Raji, C. A., Sun, P., Song, S.-K., Hershey, T., & Eisenstein, S. A. (2021).
856 Nucleus accumbens microstructure mediates the relationship between obesity and eating behavior in
857 adults. *Obesity*.

858 Samara, A., Murphy, T., Strain, J., Rutlin, J., Sun, P., Neyman, O., Sreevalsan, N., Shimony, J. S., Ances,
859 B. M., Song, S. K., Hershey, T., & Eisenstein, S. A. (2020). Neuroinflammation and White Matter
860 Alterations in Obesity Assessed by Diffusion Basis Spectrum Imaging. *Frontiers in Human*
861 *Neuroscience*, *13*. https://doi.org/10.3389/fnhum.2019.00464

862 Schur, E. A., Melhorn, S. J., Oh, S.-K., Lacy, J. M., Berkseth, K. E., Guyenet, S. J., Sonnen, J. A., Tyagi,
863 V., Rosalynn, M., De Leon, B., Webb, M. F., Gonsalves, Z. T., Fligner, C. L., Schwartz, M. W., &
864 Maravilla, K. R. (2015). Radiologic evidence that hypothalamic gliosis is associated with obesity
865 and insulin resistance in humans. *Obesity*, *23*(11), 2142–2148.
866 https://doi.org/https://doi.org/10.1002/oby.21248

867 Sewaybricker, L. E., Kee, S., Melhorn, S. J., & Schur, E. A. (2021). Greater radiologic evidence of
868 hypothalamic gliosis predicts adiposity gain in children at risk for obesity. *Obesity*, *29*(11), 1770–
869 1779. https://doi.org/https://doi.org/10.1002/oby.23286

870 Sewaybricker, L. E., Melhorn, S. J., Papantoni, A., Webb, M. F., Hua, J., Roth, C. L., Carnell, S., &
871 Schur, E. A. (2021). Pilot multi-site and reproducibility study of hypothalamic gliosis in children.
872 *Pediatric Obesity*, *16*(4), e12732. https://doi.org/https://doi.org/10.1111/ijpo.12732

873 Sewaybricker, L. E., Schur, E. A., Melhorn, S. J., Campos, B. M., Askren, M. K., Nogueira, G. A. S.,
874 Zambon, M. P., Antonio, M. A. R. G. M., Cendes, F., Velloso, L. A., & Guerra-Junior, G. (2019).
875 Initial evidence for hypothalamic gliosis in children with obesity by quantitative T2 MRI and
876 implications for blood oxygen-level dependent response to glucose ingestion. *Pediatric Obesity*,
877 *14*(2), e12486. https://doi.org/https://doi.org/10.1111/ijpo.12486

878 Shah, B., Tombeau Cost, K., Fuller, A., Birken, C. S., & Anderson, L. N. (2020). Sex and gender
879 differences in childhood obesity: contributing to the research agenda. *BMJ Nutrition, Prevention &*
880 *Health*, *3*(2), 387–390. https://doi.org/10.1136/bmjnph-2020-000074

881 Simmonds, M., Llewellyn, A., Owen, C. G., & Woolacott, N. (2016). Predicting adult obesity from
882 childhood obesity: a systematic review and meta-analysis. *Obesity Reviews*, *17*(2), 95–107.
883 https://doi.org/https://doi.org/10.1111/obr.12334

884 Smith, S. M., Jenkinson, M., Johansen-Berg, H., Rueckert, D., Nichols, T. E., Mackay, C. E., Watkins, K.
885 E., Ciccarelli, O., Cader, M. Z., Matthews, P. M., & Behrens, T. E. J. (2006). Tract-based spatial
886 statistics: Voxelwise analysis of multi-subject diffusion data. *NeuroImage*, *31*(4), 1487–1505.
887 https://doi.org/https://doi.org/10.1016/j.neuroimage.2006.02.024

888 Smith, S. M., Jenkinson, M., Woolrich, M. W., Beckmann, C. F., Behrens, T. E. J., Johansen-Berg, H.,
889 Bannister, P. R., De Luca, M., Drobnjak, I., Flitney, D. E., Niazy, R. K., Saunders, J., Vickers, J.,
890 Zhang, Y., De Stefano, N., Brady, J. M., & Matthews, P. M. (2004). Advances in functional and
891 structural MR image analysis and implementation as FSL. *NeuroImage*, *23*, S208–S219.
892 https://doi.org/https://doi.org/10.1016/j.neuroimage.2004.07.051

893 Smith, S. M., & Nichols, T. E. (2009). Threshold-free cluster enhancement: Addressing problems of
894 smoothing, threshold dependence and localisation in cluster inference. *NeuroImage*, *44*(1), 83–98.
895 https://doi.org/https://doi.org/10.1016/j.neuroimage.2008.03.061

896 Sochocka, M., Diniz, B. S., & Leszek, J. (2017). Inflammatory Response in the CNS: Friend or Foe?
897 *Molecular Neurobiology*, *54*(10), 8071–8089. https://doi.org/10.1007/s12035-016-0297-1

898 Spear, L. P. (2000). The adolescent brain and age-related behavioral manifestations. *Neuroscience &*
899 *Biobehavioral Reviews*, *24*(4), 417–463. https://doi.org/https://doi.org/10.1016/S0149-
900 7634(00)00014-2

901 Stice, E., Yokum, S., Burger, K. S., Epstein, L. H., & Small, D. M. (2011). Youth at Risk for Obesity
902 Show Greater Activation of Striatal and Somatosensory Regions to Food. *The Journal of*
903 *Neuroscience*, *31*(12), 4360 LP – 4366. https://doi.org/10.1523/JNEUROSCI.6604-10.2011

904 Stranahan, A. M., Hao, S., Dey, A., Yu, X., & Baban, B. (2016). Blood-brain barrier breakdown promotes
905 macrophage infiltration and cognitive impairment in leptin receptor-deficient mice. *Journal of*
906 *Cerebral Blood Flow and Metabolism : Official Journal of the International Society of Cerebral*
907 *Blood Flow and Metabolism*, *36*(12), 2108–2121. https://doi.org/10.1177/0271678X16642233

908 Sun, P., George, A., Perantie, D. C., Trinkaus, K., Ye, Z., Naismith, R. T., Song, S.-K., & Cross, A. H.
909 (2020). Diffusion basis spectrum imaging provides insights into MS pathology. *Neurology* -

Neuroimmunology Neuroinflammation, *7*(2), e655. https://doi.org/10.1212/NXI.0000000000000655

Tait, J. L., Collyer, T. A., Gall, S. L., Magnussen, C. G., Venn, A. J., Dwyer, T., Fraser, B. J., Moran, C., Srikanth, V. K., & Callisaya, M. L. (2022). Longitudinal associations of childhood fitness and obesity profiles with midlife cognitive function: an Australian cohort study. *Journal of Science and Medicine in Sport*, *25*(8), 667–672. https://doi.org/https://doi.org/10.1016/j.jsams.2022.05.009

Taylor, R. W., Jones, I. E., Williams, S. M., & Goulding, A. (2000). Evaluation of waist circumference, waist-to-hip ratio, and the conicity index as screening tools for high trunk fat mass, as measured by dual-energy X-ray absorptiometry, in children aged 3-19 y. *The American Journal of Clinical Nutrition*, *72*(2), 490–495. https://doi.org/10.1093/ajcn/72.2.490

Thaler, J. P., Yi, C.-X., Schur, E. A., Guyenet, S. J., Hwang, B. H., Dietrich, M. O., Zhao, X., Sarruf, D. A., Izgur, V., Maravilla, K. R., Nguyen, H. T., Fischer, J. D., Matsen, M. E., Wisse, B. E., Morton, G. J., Horvath, T. L., Baskin, D. G., Tschöp, M. H., & Schwartz, M. W. (2012). Obesity is associated with hypothalamic injury in rodents and humans. *The Journal of Clinical Investigation*, *122*(1), 153–162. https://doi.org/10.1172/JCI59660

Valdearcos, M., Douglass, J. D., Robblee, M. M., Dorfman, M. D., Stifler, D. R., Bennett, M. L., Gerritse, I., Fasnacht, R., Barres, B. A., Thaler, J. P., & Koliwad, S. K. (2017). Microglial Inflammatory Signaling Orchestrates the Hypothalamic Immune Response to Dietary Excess and Mediates Obesity Susceptibility. *Cell Metabolism*, *26*(1), 185-197.e3. https://doi.org/10.1016/j.cmet.2017.05.015

Vazquez, C. E., & Cubbin, C. (2020). Socioeconomic Status and Childhood Obesity: a Review of Literature from the Past Decade to Inform Intervention Research. *Current Obesity Reports*, *9*(4), 562–570. https://doi.org/10.1007/s13679-020-00400-2

Velloso, L. A., & Schwartz, M. W. (2011). Altered hypothalamic function in diet-induced obesity. In *International Journal of Obesity* (Vol. 35, Issue 12, pp. 1455–1465). https://doi.org/10.1038/ijo.2011.56

Verstynen, T. D., Weinstein, A. M., Schneider, W. W., Jakicic, J. M., Rofey, D. L., & Erickson, K. I. (2012). Increased body mass index is associated with a global and distributed decrease in white matter microstructural integrity. *Psychosomatic Medicine*, *74*(7), 682–690. https://doi.org/10.1097/PSY.0b013e318261909c

Wang, G. J., Volkow, N. D., Logan, J., Pappas, N. R., Wong, C. T., Zhu, W., Netusll, N., & Fowler, J. S. (2001). Brain dopamine and obesity. *Lancet*, *357*(9253), 354–357. https://doi.org/10.1016/S0140-6736(00)03643-6

Wang, X., Cusick, M. F., Wang, Y., Sun, P., Libbey, J. E., Trinkaus, K., Fujinami, R. S., & Song, S.-K. (2014). Diffusion basis spectrum imaging detects and distinguishes coexisting subclinical inflammation, demyelination and axonal injury in experimental autoimmune encephalomyelitis mice. *NMR in Biomedicine*, *27*(7), 843–852. https://doi.org/https://doi.org/10.1002/nbm.3129

Wang, Y., Sun, P., Wang, Q., Trinkaus, K., Schmidt, R. E., Naismith, R. T., Cross, A. H., & Song, S. K. (2015). Differentiation and quantification of inflammation, demyelination and axon injury or loss in multiple sclerosis. *Brain*, *138*(5), 1223–1238. https://doi.org/10.1093/brain/awv046

Wang, Y., Wang, Q., Haldar, J. P., Yeh, F.-C., Xie, M., Sun, P., Tu, T.-W., Trinkaus, K., Klein, R. S., Cross, A. H., & Song, S.-K. (2011). Quantification of increased cellularity during inflammatory demyelination. *Brain : A Journal of Neurology*, *134*(Pt 12), 3590–3601. https://doi.org/10.1093/brain/awr307

White, N. S., Leergaard, T. B., D'Arceuil, H., Bjaalie, J. G., & Dale, A. M. (2013). Probing tissue microstructure with restriction spectrum imaging: Histological and theoretical validation. *Human Brain Mapping*, *34*(2), 327–346. https://doi.org/https://doi.org/10.1002/hbm.21454

Willette, A. A., & Kapogiannis, D. (2015). Does the brain shrink as the waist expands? *Ageing Research Reviews*, *20*, 86–97. https://doi.org/10.1016/j.arr.2014.03.007

Winkler, A. M., Ridgway, G. R., Webster, M. A., Smith, S. M., & Nichols, T. E. (2014). Permutation inference for the general linear model. *NeuroImage*, *92*, 381–397. https://doi.org/https://doi.org/10.1016/j.neuroimage.2014.01.060

Winklewski, P. J., Sabisz, A., Naumczyk, P., Jodzio, K., Szurowska, E., & Szarmach, A. (2018). Understanding the physiopathology behind axial and radial diffusivity changes-what do we Know? In *Frontiers in Neurology* (Vol. 9, Issue FEB). Frontiers Media S.A. https://doi.org/10.3389/fneur.2018.00092

Wisniewski, A. B., & Chernausek, S. D. (2009). Gender in childhood obesity: Family environment, hormones, and genes. *Gender Medicine*, *6*, 76–85. https://doi.org/https://doi.org/10.1016/j.genm.2008.12.001

World Health Organization. (2021). *Obesity and overweight*. https://www.who.int/en/news-room/fact-sheets/detail/obesity-and-overweight

Wu, C., Garamszegi, S. P., Xie, X., & Mash, D. C. (2017). Altered Dopamine Synaptic Markers in Postmortem Brain of Obese Subjects . In *Frontiers in Human Neuroscience* (Vol. 11, p. 386). https://www.frontiersin.org/article/10.3389/fnhum.2017.00386

Yang, R., Lin, T.-H., Zhan, J., Lai, S., Song, C., Sun, P., Ye, Z., Wallendorf, M., George, A., Cross, A. H., & Song, S.-K. (2021). Diffusion basis spectrum imaging measures anti-inflammatory and neuroprotective effects of fingolimod on murine optic neuritis. *NeuroImage. Clinical*, *31*, 102732. https://doi.org/10.1016/j.nicl.2021.102732

Yendiki, A., Koldewyn, K., Kakunoori, S., Kanwisher, N., & Fischl, B. (2014). Spurious group differences due to head motion in a diffusion MRI study. *NeuroImage*, *88*, 79–90. https://doi.org/10.1016/j.neuroimage.2013.11.027

Zhan, J., Lin, T.-H., Libbey, J. E., Sun, P., Ye, Z., Song, C., Wallendorf, M., Gong, H., Fujinami, R. S., & Song, S.-K. (2018). Diffusion Basis Spectrum and Diffusion Tensor Imaging Detect Hippocampal Inflammation and Dendritic Injury in a Virus-Induced Mouse Model of Epilepsy . In *Frontiers in Neuroscience* (Vol. 12, p. 77). https://www.frontiersin.org/article/10.3389/fnins.2018.00077